energies

MDPI

Article

Mining-Induced Seismicity during Development Works in Coalbeds in the Context of Forecasts of Geomechanical Conditions

Dariusz Chlebowski * and Zbigniew Burtan

Faculty of Civil Engineering and Resource Management, AGH University of Science and Technology, Mickiewicza 30 Av., 30-059 Cracow, Poland; burtan@agh.edu.pl
* Correspondence: chlebo@agh.edu.pl

Abstract: Mining-induced seismicity in the area of development works and proper mining operations is one of the major determinants of the rockburst hazard level in underground mines. Rockburst hazard assessment in Polish collieries is performed by a variety of mining and geophysical methods, including seismic and seismoacoustic techniques, borehole surveys, small diameter drilling, rock strata profiling and analyses of geomechanical properties of rocks, geological structure and geological mining conditions. In the case of zones particularly exposed to potential hazards, it is recommended that analytical or numerical forecasts of the state of stress in the vicinity of workings should be used already at the stage of planning of mining operations. This study summarises the comparative analysis of seismic test data and analytical forecasts of the state of stress in five selected headings in one of the burst-prone collieries within the Upper Silesia Coal Basin in Poland (USCB). As regards the seismic data, duly defined quantitative indicators and energy criteria of the registered seismic activity are recalled in the assessment of rockburst hazard level during the roadheading operations. Analytical simulations utilise a developed geomechanical model and stress–strain relationships stemming from the principles of elastic media mechanics. From the standpoint of mining engineering practice, interpretation of results obtained by the two methods reveals how effective analytical models will be in prognosticating or verification of rockburst hazard conditions.

Keywords: rockburst hazard; mining-induced seismicity; rock mechanics; analytical modelling

Citation: Chlebowski, D.; Burtan, Z. Mining-Induced Seismicity during Development Works in Coalbeds in the Context of Forecasts of Geomechanical Conditions. *Energies* **2021**, *14*, 6675. https://doi.org/10.3390/en14206675

Academic Editor: Waldemar Korzeniowski

Received: 7 September 2021
Accepted: 7 October 2021
Published: 14 October 2021

1. Introduction

In intact rock mass, the rock strata remain in natural stable mechanical equilibrium conditions [1–3]. Underground mining operations will disturb this equilibrium, triggering the rockburst occurrence (seismic events generating energy in excess of 10 J and producing vibrations with frequency below 100 Hz [4]). From the standpoint of geomechanics, rockbursts are regarded as the rock strata response to variations of stress and elastic energy distribution in the vicinity of mine excavations. On account of its direct association with rockburst hazard, induced seismicity has received a great deal of attention from rock engineering practitioners at geophysical stations in mines, mine supervision authorities as well as research institutes [5]. In terms of effectiveness of the solutions, the most difficult issue to be addressed is the forecasting of seismic activity levels during the preparatory and mining works. In general terms, a forecast or a rational prognosis of future processes/phenomena consists in predicting the magnitude (scale) of an upcoming event, as well as where and when it is to be anticipated. In relation to rockbursts, it is a widely shared view that a scientific approach and practical experience allow the place (area) of a seismic event and the associated energy release to be approximated, with a greater or lower accuracy. For objective reasons, a fully accurate prediction of when the next outburst will occur still remains a distant goal [6–9].

Development of monitoring systems allows us a better insight into the processes taking place within the rock medium, resulting in attempts to obtain more reliable assessment methods and predictions of seismic hazards [10,11]. Several dedicated methods have thus been recommended, including the probabilistic seismic hazard analysis [12,13], the linear predictions of aggregated seismic or seismoacoustic energy [14] or the method based on indicator functions [15]. The aspects that were subject to modifications included the criteria of interpretation and ongoing seismic hazard assessment based on selected seismic parameters associated with the analyses of epicentre mechanisms, the Gutenberg–Richter distributions, amplitudes of rock strata vibration velocity (PPV) and tomographic images of seismic wave velocity fields [16–19]. Recently, methods relying on artificial intelligence and machine learning have received a great deal of attention and gained much popularity [20–23].

Alongside the prevailing state of stress and geomechanical parameters of the rock strata, seismicity of the rock mass is a major determinant of the rockburst hazard in underground mining excavations. Rockburst hazard (potential and real) is routinely assessed in coal mines operated in Poland using a variety of monitoring techniques (seismic and seismoacoustic monitoring, borehole surveys), alongside the rigorous study of the mining conditions at the stage of planning of the mining activities [4,24]. In most complex geological and mining settings, mine practitioners resort to other methods as well, including expert mathematical modelling (analytical or/and numerical techniques) [25]. They facilitate the collection or verification of data on the extent and magnitude of anomalies, i.e., zones of stress concentrations or destressed zones within the rock strata, in the context of the projected layout of mine headings and production workings.

In the vast majority of coal mines in the USCB that are still operational, coal mining is continued from deep seams and in confined conditions associated with the presence of remnants from previous mining operations, from geological disturbances or compact sandstone features or sandy shale formations. Consequently, high-energy mining-induced seismicity increases the risk of potential rockbursts in underground mines [26]. In terms of geomechanical engineering, the presence of constraining factors leads to changes in the state of stress and, consequently, in the density of elastic strain energy in the surrounding rock strata, affecting both overlying and underlying coal seams as well as the strata that are potentially burst-prone and likely to give rise to dynamic critical stress changes involving the fracturing of coal and/or roof strata (destruction of their original structure). Consequently, low-energy seismic activity will increase (its foci at close range, located within the coalbed or in the immediate roof of floor strata); alternatively, high-energy seismicity will be intensified (its foci far distant, located in the main roof strata).

This study investigates mining-induced seismicity during development works in mine workings and headings, in the context of reliability of the state of stress forecasts based on analytical simulation data. The test field was a coalbed section (panel Y, coal seam 409-4) in one of the collieries within the Upper Silesia Coal Basin [27]. Five selected headings were considered, which were drifted for the purpose of contouring and to provide the required ventilation and haulage facilities for future mining operations in two longwall panel sections (Y/2, Y/4). Underpinned by the fundamental objectives of mining seismology: monitoring, recording and analysis of rockburst events [28–31], the seismic events registered while the respective headings were driven were duly reviewed and synthesised. Reports of mining-induced seismic events registered during underground mining operations (in coal mines and elsewhere) can be found in literature on the subject of mining conditions in Poland [32–35], the Czech Republic [36], USA [37], China [38], South Africa [39], Australia [40] and elsewhere [41–44]. The input data were the locations of registered events and duly defined parameters (criterial indicators) highlighting the quantitative aspects and energy potentials of registered seismicity. Results of seismic analyses were then examined, in consideration of forecasted locations of zones featuring anomalous variations of the vertical stress component and stress concentration factor, obtained by analytical modelling. The modelling procedure relies on the modified solution

offered by mechanics of deformable media [2,3,45,46], having relevance to the stress–strain conditions within coalbeds. The theory of elasticity is commonly recalled to determine and analyse the state of stress, the critical stress and energy processes occurring within the rock strata and triggered by mining operations [47–50]. Underlying the stress forecasts in the present study is the theory of bending plates rested on an elastic surface [2,51].

2. Materials and Methods

2.1. Geological and Mining Conditions in the Investigated Area

The area of concern included the panel Y within the coalbed 409-4 which is planned to be worked on by operating two longwall panel sections (Y/2, Y/4) in the serial home-mining sequence, the working face advancing from the south northwards. To provide for ventilation and transport facilities, the required development mining operations were completed (Figure 1, blue contour line), involving the opening out of the main workings (within the coal seam and in the barren rock strata) in the parallel configuration (their larger parts situated in the pillar zone protecting the drift F on the level 900 m) and longitudinally arrayed butt headings as well as the system of interconnecting cross headings (cut in coal). On account of the presence of residues of previous mining excavations, involving the excavation limits of the coalbeds 409-3 (vertical distance 6–19 m) and 406-1 (vertical distance 150–160 m), the heading Y#10 had to be driven, alongside the downcast gate Y#2, the top heading Y#2 and bottom heading Y#4.

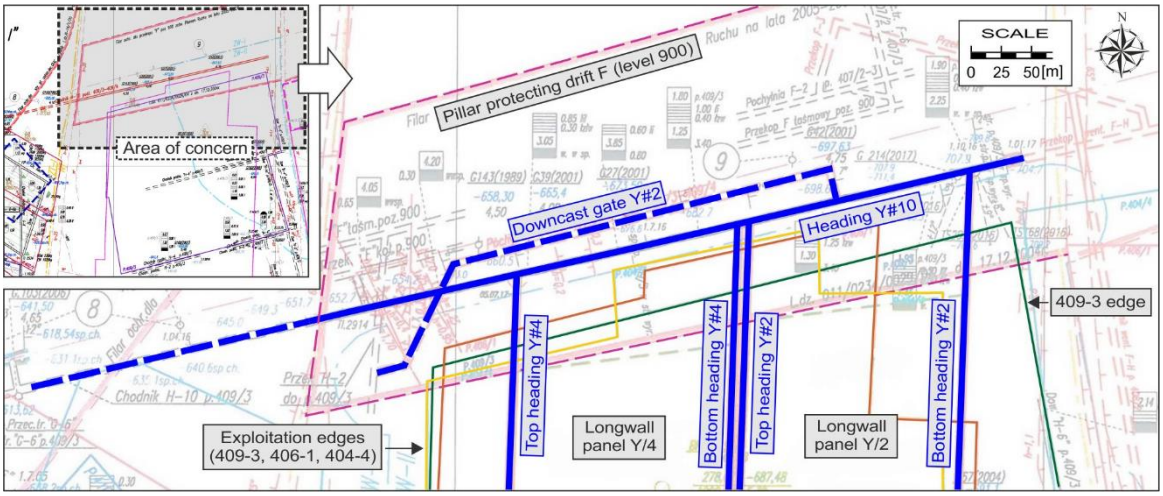

Figure 1. Coal seam section in the area of concern.

The investigated panel is enclosed on the eastern and western side by two major faults with the thrust of 15–25 m, accompanied by minor tectonic features, their amplitudes locally exceeding 5 m. The thickness of the coalbed 409-4 falls in the range 4.0–5.3 m, at the depth of 820–980 m. The lithologic profile of the surrounding strata is dominated by sandy shale features and thick sandstone strata, which were identified by geological drilling (geophysical logs) in the course of development mining and coal extraction from overlying coal seams (406-1, 408-2, 409-3). Sandy shales separating coal seams 409-3 and 409-4 (about 20 m thick in the north-west section) are gradually replaced by clay shales, their thickness being reduced to 1 m (or 0.3 m locally) along the east-south direction. The actual inclination of strata is varied, ranging from 5 to 12°/E and whilst clay shales feature slaty cleavability, sandstones and sandy shales display slaty as well as block cleavability whilst coals have cubical cleavages. Penetrometric test data show that the uniaxial compressive strength (Rc) of coal from the seam 409-4 is approximately equal to 11.8 MPa (the tensile strength being 0.4 MPa). For clay shales, Rc ranges from 21 to 42.3 MPa, for sandy shales it is 36.5–70.9 MPa, whilst the uniaxial compressive strength of sandstone is found to be 52.2–103.7 MPa.

To date, no mining operations have been conducted in the analysed section of the panel Y in the coal seam 409-4 in the zone to the south of the pillar protecting the drift F (at the level 900), though in the past (1980–2007) coal used to be extracted from the neighbouring level-300 seams (363) and level-400 seams (401-2, 403-1, 404-2, 404-4, 406-1 and 409-3). In most cases, the longwall mining system was deployed, following the nearly longitudinal pattern (the only exception being two transverse longwall faces operated in the coal seam 409-3, with roof control through caving in (locally backfilled). Based on available source documents, it is reasonable to suppose that although the range of vertical distances (in the cross-profile) of respective coal seams with respect to the coal seam 409-4 is considerable (6–380 m), the estimated total thickness of the extracted layer in the investigated panel section Y will locally approach 40 m [27].

2.2. Objectives of Seismic Activity Evaluation

The geophysical station in the mine is responsible for ongoing real-time monitoring of seismic activity. The monitoring is based on a seismologic system providing for digital data transmission and relying on the network of seismometers and uniaxial or triaxial sets of geophones. The system is supported by dedicated software affording us the means to detect seismic events, their locality and energy potential, and allowing the data to be archived on an online basis.

The starting point for further analyses was a total tally of seismic events registered during the drifting operations whilst the final database was restricted to seismic events with energy release of 1.0×10^2 J or more (Table 1).

Table 1. Record of seismic events.

Date	H	M	S	x	y	z	Energy	Panel Section	Coalseam	Excavation	Additional Remarks
1 May 2018	7	36	21	−49,690	−16,560	−620	2.2×10^4	Y	409-4	bottom heading Y#2	
17 July 2017	0	45	52	−49,760	−16,950	−660	1.7×10^3	Y	409-4	top heading Y#4	SU
29 June 2017	23	44	11	−49,780	−16,950	−640	6.3×10^4	Y	409-4	top heading Y#4	
8 April 2018	11	31	52	−49,640	−16,580	−710	3.4×10^2	Y	409-4	bottom heading Y#2	
10 March 2018	4	17	28	−49,740	−16,880	−670	5.0×10^3	Y	409-4	heading Y#10	
30 April 2018	10	57	19	−49,750	−16,760	−660	9.4×10^2	Y	409-4	bottom heading Y#4	ST

H, M, S—exact time of the event (hours, minutes, seconds); x, y, z—coordinates of the burst hypocentre; SU—destress blasting; ST—torpedo blasting.

In the first stage, the data were collated and classified accordingly in the light of the adopted criteria: type of excavation, the time of event occurrence, energy potential, epicentre (foci) coordinates and adopted active rockburst control measures. Finally, the seismic events were categorised as spontaneous or induced, whilst the time frame of individual events and their foci locations were determined separately for each investigated heading.

Further analysis and evaluation of seismic hazard were based on selected parameters of mining-induced rock mass activity, including:

- Total number of registered events, N (-);
- Total energy release, As (J);
- Average energy released in a single tremor, As/N (J);
- Average rate of working face advance (m) per a single tremor, W1 (m/1 tremor); and
- Average energy generated per 1 m of the working face advance, W2 (J/m).

Another aspect of concern was the focus location with respect to the headings being driven. According to the data supplied by the mining companies, the error involved in

positioning of horizontal (epicentre) coordinates x, y was less than 25 m for the investigated working. To demonstrate the effectiveness of the adopted active rockburst control measures, the quantitative inducibility factor PN (%) was recalled, expressed as the ratio of the number of blasting-induced tremors (registered within the post-blast waiting time) (Nw) to the total number of events registered during the drifting operations (N).

2.3. Main Objectives of Geomechanical Assessment of Seismic Activity and Rockburst Hazard

Generally, rockbursts in mines are regarded as dynamic phenomena triggered by quakes and tremors in rock strata, resulting in damage or destruction of the mine workings (or their sections) in such a degree that further mining operations are either impossible or vastly limited, or the safety features have significantly deteriorated. Tremors in rock strata are associated with rapid release of accumulated potential energy in a process involving rock mass vibrations, air shock waves as well as acoustic phenomena. Potential incidence of a tremor or rockburst as a consequence of unfavourable geological and mining conditions has remained the key criterion in rockburst hazard evaluation in underground mines [52]. A necessary condition triggering the rockburst occurrence in an underground heading is the fracturing of the surrounding rock strata due to the critical stress loads in certain areas of the coal seam [51,53]. The stress arising in the rock strata as a consequence of deformation processes can be expressed by a stress indicator, and recalling the Mohr–Coulomb criterion it can be defined as the function of strength parameters and principal stresses [3,54]. The magnitudes of the state of stress components in the investigated coal seam are determined, in turn, by its depth, the impacts of residual features and tectonic disturbances; moreover, they also depend on the employed mining method and working technology, as well as type and geometry of headings [55–57].

In the context of modelling deformations and stress conditions in the rock strata, mathematical methods (analytical or numerical) have gained in importance in the long-term design of mining operations. They can be used in mine engineering practice to determine (estimate) the magnitude of rockburst hazard during mining and drifting operations. Apart from geomechanical factors, the actual scale of hazard is dependent on the state of stress in the vicinity of mining excavations, hence this evaluation relies on analytical simulation data yielding the variability patterns of the following parameters:

- Vertical component of the primary stress (σ_z), as a superposition of gravity-induced stresses (p_z), stresses caused by the presence of residues of previous mining operations (p_k) and by impacts of geological disturbances and bedding irregularities (p_t):

$$\sigma_z = p_z + p_k + p_t \tag{1}$$

- Stress concentration factor (k), expressed as the quotient of primary vertical stresses (σ_z) and lithostatic stresses (p_z):

$$k = \frac{\sigma_z}{p_z} \tag{2}$$

The geomechanical model of the rock strata was recalled (Figure 2), underpinned by the theory of plate bending on deformable substrate [2,51]. The model provides for approximated nonlinearity of the coal bed (seam) characteristic and linear deformability of roof/floor strata whilst the constraints due to confined work conditions are represented by non-uniform distribution of external static loads ($p(x)$) [53]. Parameters of merit include the modulus of elasticity of coal, roof and floor strata (E_w, E_{str}, E_{sp}), coalbed thickness and post-failure modulus of coal (h_w, M_w), inertia moment of the roof and floor panel cross-section with respect to a neutral axis (J_{str}, J_{sp}) and equivalent bending rigidity of an equivalent system (EJ). The applied algorithm uses predefined differential equations of the equivalent roof plate bending line in relation to particular model components (including the working space, intact coal rock), given as:

$$A\,\frac{d^4 w_i(x)}{dx^4} + B\,w_i(x) + p(x) + C = 0 \tag{3}$$

where:

$w_i(x)$—displacement function (for model components),
$p(x)$—external load function,
A, B, C—constant coefficients.

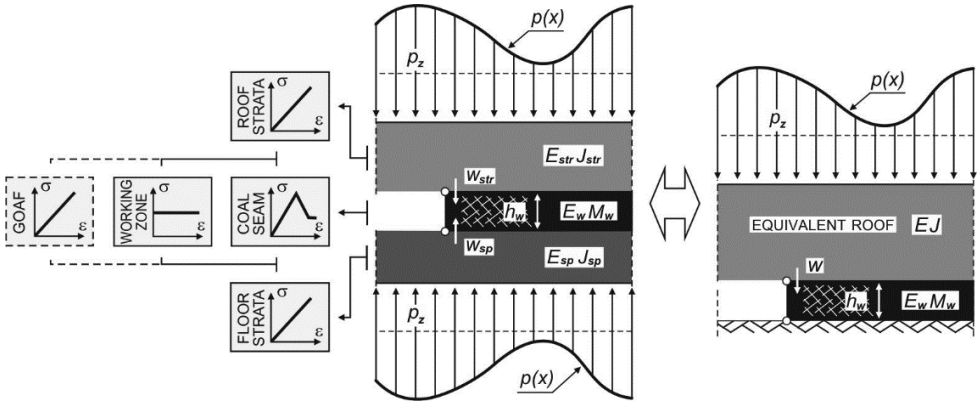

Figure 2. Geomechanical model of the rock strata.

Taking into account the potential of disintegration of the original coalbed structure, the respective system of heterogeneous linear equations was solved accordingly, recalling the boundary conditions for bending, inclination and internal forces acting on characteristic points. Thus, obtained formulas governing the distributions of displacements ($w = f(w_{str}, w_{sp})$) and vertical stresses (σ_z) within the coalbed were then implemented, largely in the form of numerical procedures, in a dedicated computer program developed by the authors. The mechanical parameters of the rock strata and information on the local mining conditions in the area of concern (including the impacts of previous mining operations) being entered, the calculation procedure was applied using the Cartesian coordinate system (emulating the geometry of the panel Y), with a step guaranteeing sufficient accuracy (basic grid 5 m × 5 m). Calculation results were given in the form of contour maps illustrating the variability of parameters expressed by the Formulas (1) and (2).

3. Results

3.1. Seismic Activity during the Drifting Operations

At the time this study was conducted, development mining works in the area of concern were still underway with six headings (totalling 2.6 km in length) being completed partly or as a whole. Apparently, 99.9% of 850 seismic events totalling 4.98×10^6 J registered during the drifting stage had the energy potential of 10^2–10^4 J (minor events of the order of 10^1 J being neglected). A single high-energy tremor registered (1.5×10^5 J) in conjunction with the driftage of the downcast gate Y#2 seems to have been triggered by active rockburst control measures in the form of torpedo blasting in the roof strata. None of the recorded tremors seems to have produced negative impacts on mine workings.

In consideration of the scope of the driftage operations, the main focus was on the selected five headings having the total length of about 2.4 km. More detailed information on the applied roadheading technology, direction of respective headings and the state of progress of roadheading works as of the day the study was conducted (the available database of seismologic data) is summarised below:

- Heading Y#10 (coal seam 409-3/4); direction of drift advance: eastwards; working method: mechanical working (roadheader) and traditional methods (use of explosives); progress status: fully completed (839 m, 100%);
- Downcast gate Y#2 (coal seam 409-3/4); driftage direction: eastwards; working method: mechanical working (roadheader) and traditional methods (use of explosives); progress status: fully completed (486 m, 100%);

- Top heading Y#4 (coal seam 409-4); driftage direction: southwards; working method: mechanical working (roadheader) and traditional methods (use of explosives); progress status: fully completed (550 m, 100%);
- Bottom heading Y#4 (coal seam 409-4); two driftage directions: the northward segment; working method: mechanical working (roadheader) and traditional methods (use of explosives); progress status: partially completed (507 m, ~93%); and the southward segment; working method: traditional methods (use of explosives); progress status: partially completed (5 m, ~13%);
- Bottom heading Y#2 (coal seam 409-4); driftage direction: southwards; working method: traditional methods (use of explosives); progress status: partially completed (21 m, ~4%).

Heading Y#10. In the course of drifting operations, seismic activity remained on the medium level (in relation to other face zones). Out of the total number (N = 142) of registered tremors (126 spontaneous and 16 mining-induced events) with the total energy release 5.05 × 10^5 J (As), there were 34 tremors (23.9% of the population) with the energy ratings of the order of 10^2 J, 106 tremors (74.7%) with 10^3 J and 2 tremors (1.4%) with the energy potential of the order of 10^4 J. The foci would be fairly uniformly distributed with respect to direction of driftage in the vicinity of the face and intact coal rock on both the northern and eastern part of the roadside, except for two segments situated within the zone of the projected crossing with the bottom heading Y#4 (top heading Y#2) and to the east of the crossing with the bottom heading Y#2 (Figure 3). Taking into account the total length of the excavation (839 m), it is reasonable to estimate that a statistical tremor with the average energy potential of 3.56 × 10^3 J (As/N) would be registered with every 5.9 m of the work advance (W1) and energy released per one running metre of the heading would be 6.02 × 10^2 J (W2). The actual value of the quantitative parameter referred to as inducibility of seismic events (PN), regarded as an indicator related indirectly to effectiveness of active rockburst control measures (destress blasting), was equal to 11.3%, encompassing all tremors with the energy ratings 10^2–10^3 J.

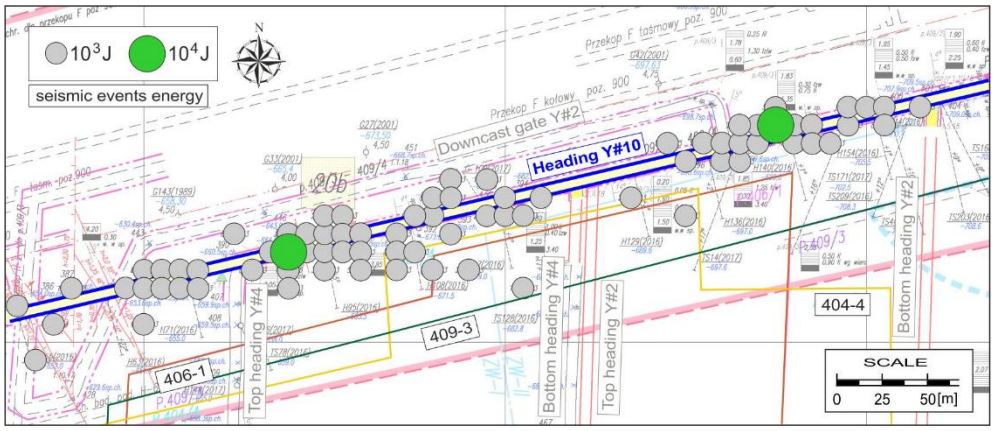

Figure 3. Distribution of seismic events with energy E ≥ 10^3 J during the drifting of heading Y#10.

Downcast gate Y#2. Seismic activity registered during the drifting operations was on a relatively high level, the highest among other workings. Out of the total number (N) of 480 recorded tremors (427 spontaneous and 53 mining-induced events) with the total energy release 2.5 × 10^6 J (As), 88 tremors (18.3% of the population) had the energy potential of the order of 10^2 J, 367 tremors (76.5%) had 10^3 J and 24 tremors (5%) had energy of the order of 10^4 J whilst 1 (0.2%) registered tremor was of the order of 10^5 J. Actually, seismic activity was recorded in the entire face range area, throughout the whole drifting operation starting from the work commencement, the first tremor of the order of 10^3 J being reported a few days after this date. The distribution of foci with respect to directional axis of the heading was not uniform. Whilst most of them were situated in the vicinity of the

working face zone, the vast majority were found in the coal body on the right side wall, in the belt-shaped coalbed section abutting the previously driven heading Y#10 (Figure 4). Taking into account the total length of the excavation (486 m), it is reasonable to estimate that a statistical tremor with average energy of 5.21×10^3 J (As/N) would be registered with every 1 m of the work advance (W1). Energy generated per one running metre of the downcast gate was 5.14×10^3 J (W2). In quantitative terms, inducibility of seismic events (PN) was equal to 11.0% and covered the entire spectrum of energies of recorded tremors (the energy ratings 10^2–10^5 J). The applied active rockburst prevention measures included the use of coal working explosives, destress blasting and torpedo blasting (using a single blast hole).

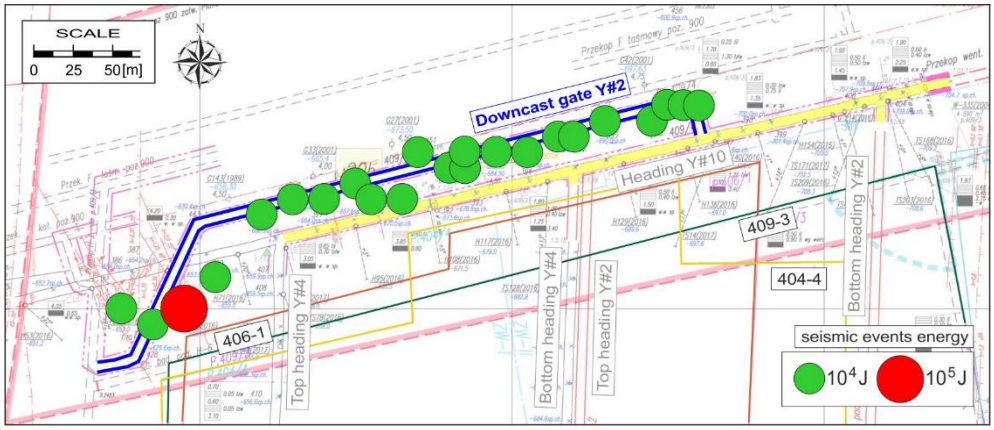

Figure 4. Distribution of seismic events with energy E $\geq 10^4$ J during the drifting of downcast gate Y#2.

Top heading Y#4. Seismic activity registered during the drifting operations remained on a relatively high level. Out of the total number (N) of 101 recorded tremors (59 spontaneous and 42 blasting-induced events) with the total energy release 1.32×10^6 J (As), 12 tremors (11.9% of the population) had the energy potential of the order of 10^2 J, 65 tremors (64.4%) had 10^3 J and 24 tremors (23.7%) had energy of the order of 10^4 J. Full-range seismic activity manifested itself soon after the drifting works commenced, starting from the crossroads with the heading Y#10 and ceasing on reaching the edges of the previously worked coal seams 406-1 and 409-3. Along the face range segment underneath the goafs (409-3) the registered seismic events were few and far between, having the energy potential of the order of 10^2–10^3 J. In the initial segment of the heading (unrelieved stress zone), the foci distribution was largely uniform along the direction the heading was driven, in the vicinity of the front face zone (in front of and behind the working face) and in the unmined coal body on both the eastern and western roadside (Figure 5).

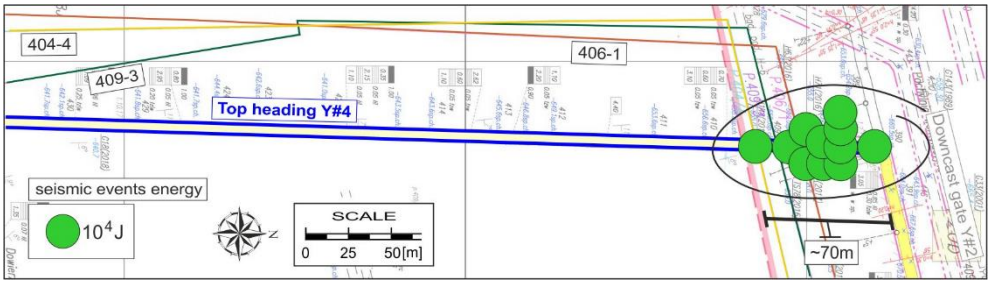

Figure 5. Distribution of seismic events with energy E $\geq 10^4$ J during the drifting of top heading Y#4.

Taking into account the total length of the excavation (550 m), it is reasonable to estimate that a statistical tremor with an average energy release of 1.31×10^4 J (As/N) would be registered with every 5.4 m of the work advance (W1). Energy generated per one

running metre of the road driven was found to be 2.40×10^3 J (W2). It is worthwhile to mention that the results given would be much less favourable if the real, enhanced seismic activity registered alongside the initial section of the working face range was taken into account. Quantitative analyses and energy calculations based on detailed work schedules and tremor records reveal the increased incidence of seismic events in conjunction with roadheading works in the first 70 m long segment of the heading: 86 events were registered (85.1% of the total number of 101 recorded tremors) of 10^2–10^3 J, with energy release 1.28×10^6 J (96.9% of the total energy release of 1.32×10^6 J). It is estimated, therefore, that a seismic event within this area would be registered every 0.8 m of the roadheading work advance, on the average ($W1^{70m}$) and the generated energy per one running metre of the heading would become 1.83×10^4 J ($W2^{70m}$). In quantitative terms, inducibility of seismic events (PN) was 41.6%, covering the tremors in all registered energy categories (10^2–10^4 J). Active rockburst control methods included the use of explosives throughout the roadheading operations, working by blasting (periodically, with additional blast holes provided in near-roof shale strata), destress blasting (periodical, with additional blast holes 5 m in length) and torpedo blasting (using one or two blast holes).

Bottom heading Y#4. Even though the roadheading operations were scheduled to involve two stages (drifting in the northward and southward directions), the heading was basically driven along the northern direction. In the meantime, a crossing was completed leading off the heading Y#10, as well as an entry to the bottom heading Y#4 in the southward direction to the depth of 5 m; after that the works were discontinued. When the heading advanced 507 m in the northward direction, the decision was made to discontinue the further driftage northwards on account of the enhanced seismic hazard/rockburst risk (most probably due to negative impacts of remnants of previous mining operations in overlying strata) and attempts were made to scallop the face (over the length of 32 m) from the end of the previously worked entry off the heading Y#10. As of the day this study was conducted, the circumstances were such that no roadheading operations continued in the northward direction whilst the further roadheading works in the southward direction were not commenced. Preparatory operations prior to roadheading in the southward direction included only torpedo blasting (later found to be most effective) using a single blast hole 35 m in length, inclined at 45% in the vertical from the heading axis.

In the course of roadheading works in the bottom heading Y#4 the seismic activity level would vary. Out of the total number (N) of 83 recorded tremors (71 spontaneous and 12 blasting-induced events) with the total energy release 5.34×10^5 J (As):

- Sixty-one events (including seven blasting-induced tremors) with the total energy release 4.21×10^5 J are assumed to have occurred in conjunction with the roadheading operations in the northward direction;
- Twenty-two events (including five blasting-induced tremors) with the total energy release 1.13×10^5 J are assumed to have occurred in conjunction with the roadheading operations in the southward direction.

Out of the total 83 recorded tremors, 28 events (33.7% of the entire population) had energy potential of the order of 10^2 J, 51 tremors (61.5%) had 10^3 J and 4 tremors (4.8%) had energy of the order of 10^4 J. Similar to the top heading (Y#4), the majority of recorded events occurred in conjunction with drifting operations in the unrelieved part of the coal seam. Along the face range segment underneath the old goafs 409-3 (in the course of drifting in the northward direction) the registered tremors were few and far between, in the energy category 10^2–10^3 J only. In the unfinished heading segments (both in the northward and southward direction) where seismic activity was most intense (between the heading Y#10 and the south end of the pillar protecting the drift F), the foci distribution would be roughly uniform with respect to the roadheading direction, in the vicinity of the working end (primarily in front of the working face) and in intact coal strata on both the eastern and western roadside. Taking into account the total length of the heading (512 m), including 507 m long segment drifted in the northward direction and 5 m directed southwards, it is reasonable to estimate that a statistical tremor with the average energy

release of 6.43 × 10^3 J (As/N) would be registered with every 6.2 m of the work advance (W1), on average. Energy generated per one running metre of the road driven would be 1.04 × 10^3 J (W2). Applying the identical calculation procedure as that adopted to analyse seismic activity in the top heading, it is reasonable to assume that enhanced seismicity would occur during the drifting of the bottom heading Y#4 northwards, along the ultimate segment of the face range (25–28 m in length) or during the completion of the entry (5 m), from the heading Y#4 southwards (Figure 6). Out of the total number of 83 recorded tremors, 64 events (77.1% of the entire population) had energy of the order of 10^2–10^4 J, with the total energy release 4.90 × 10^5 J (91.7% of events with the total energy release 5.34 × 10^5 J). It appears that along the analysed segment, having the total length of 30 m, a tremor would be recorded every 0.5 m of working end advance ($W1^{30m}$) and the energy generated per one metre of driven heading would equal 1.63 × 10^4 J ($W2^{30m}$). In quantitative terms, the average inducibility of seismic events (PN) for both working faces within the face range zone would be 14.5%, including:

- Drifting in the northward direction, including only the seismic events in the energy categories 10^2–10^3 J (three tremors with the energy rating 10^4 J were all spontaneous)—11.5%;
- Drifting in the southward direction, covering seismic events in all registered energy categories (10^2–10^4 J)—22.7%.

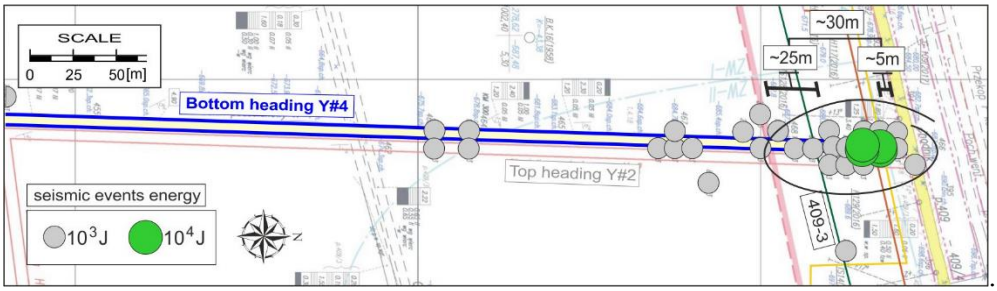

Figure 6. Distribution of seismic events with energy E ≥ 10^3 J during the drifting of bottom heading Y#4.

Active rockburst prevention measures included working by blasting (during the drafting in the northwards direction) and torpedo blasting (in the southward direction).

Bottom heading Y#2. The analysis of rock strata seismic activity in conjunction with the drifting of the bottom heading Y#2 will not be complete and fully reliable because the extent of works was rather small (21 m) in relation to other working faces. Out of the total number (N) 43 recorded tremors (26 spontaneous and 17 blasting-induced events) with the total energy release 1.25 × 10^5 J, 13 tremors (30.2% of the entire population) had energy potential of the order of 10^2 J, 30 events (69.8%) had 10^3 J and no events were recorded in the energy category 10^4 J. Seismic activity occurred immediately after the roadheading works commenced (starting from the crossing with the heading Y#10) and levelled off throughout the entire drifting operation. The foci were fairly uniformly distributed along the direction of the working face advance, in the vicinity of the face end (in front of the working face) and in intact coal strata on both eastern and western roadsides (Figure 7). Taking into account the total length of the driven heading (21 m), it is reasonable to estimate that a statistical tremor with the average energy release of 2.91 × 10^3 J (As/N) would be registered with every 0.5 m of the work advance (W1) and the generated energy per one running metre of the heading would be 6.10 × 10^3 J (W2). In quantitative terms, inducibility of seismic events (PN) as a parameter related indirectly to effectiveness of active rockburst control measures (working by blasting) was equal to 39.5%, including all tremors with energy ratings 10^2–10^3 J.

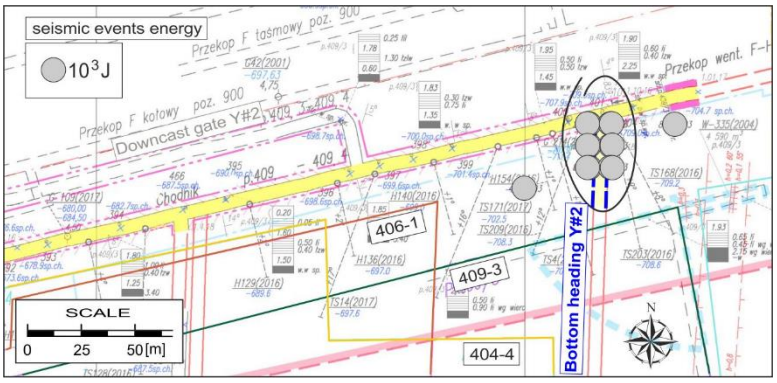

Figure 7. Distribution of seismic events with energy E $\geq 10^3$ J during the drifting of bottom heading Y#2.

3.2. Seismic Risk Evaluation in the Light of Stress Forecasts

Forecasted data are presented as contour maps of vertical stress (σ_z) and stress concentration factor (k) (see Figures 8 and 9) in the fragment of panel Y within the coal seam 409-4 (Figure 1). The simulation procedure was conducted at the stage of work planning, prior to the commencement of development drifting and mining (Figures 8 and 9, blue contour), revealing a non-uniform distribution of the state of stress in the analysed section of panel Y, largely attributable to impacts of previous mining excavations in overlying strata. Simulation data lead us to the following conclusions:

- Variability range of the vertical stress component (σ_z) in the region of mine workings is wide, ranging from 19.5 to 41.4 MPa (Figure 8);
- There are both destressed zones where the stress concentration factor (k) is in the range 0.79–1.0, alongside stress concentration zones where the value of k becomes as high as 1.68 (Figure 9).
- The most unfavourable stress conditions (of 30 MPa or more) prevail in the belt-shaped section of intact coal rock abutting the edge coinciding with the boundary of mined-out goafs in the coal seam 409-3; the impacts of remnants of previous mining operations in the coal seam 406-1 (and overlying) are relatively insignificant;
- In terms of critical stress analysis, the location of the heading Y#10 (coal seam 409-4) and the downcast gate Y#2 (in the coal seam 409-3/4) is quite favourable because the actual values of the vertical stress component and stress concentration factor along the face range only slightly differ from the lithostatic stress conditions (of the order of 24.2 MPa);
- Segments of the top headings (Y#4, Y#2) and of the bottom heading (Y#2) from the crossing with the heading Y#10 to the southern end of the pillar protecting drift F experience most unfavourable stress conditions due to the transverse edge of a goaf in coal seam 409-3.

It is worthwhile to mention that in the entire analysed region, even in potentially stress-relieved zones, the obtained minimal values of vertical stress in the coal seam (19.5 MPa, see Figure 8) are higher (significantly higher, locally) than the instantaneous uniaxial compression strength of coal in the seam 409-4 (below 12 MPa). These conditions give rise to the critical stress zones, or lead to formation of more or less extensive fracturing zones. That means that at the stage of roadheading (and during mining operations), the conditions will prevail that enhance the risk of low-energy tremors (of the order of 10^3 J and 10^4 J), their foci in the coal rock or in immediate roof or floor strata. A growing number of such events (alongside the increased rockburst risk), is to be expected, particularly in conjunction with elevated stress zones in segments of all headings (Y#2, Y#4) in the belt-shaped area between the edge of 409-3 and the heading Y#10.

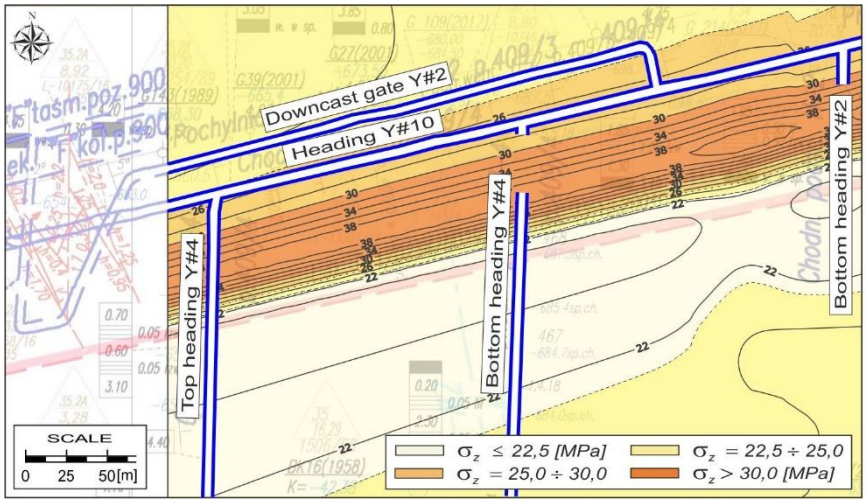

Figure 8. Vertical stress contour (σ_z) in the coal seam (within the panel Y).

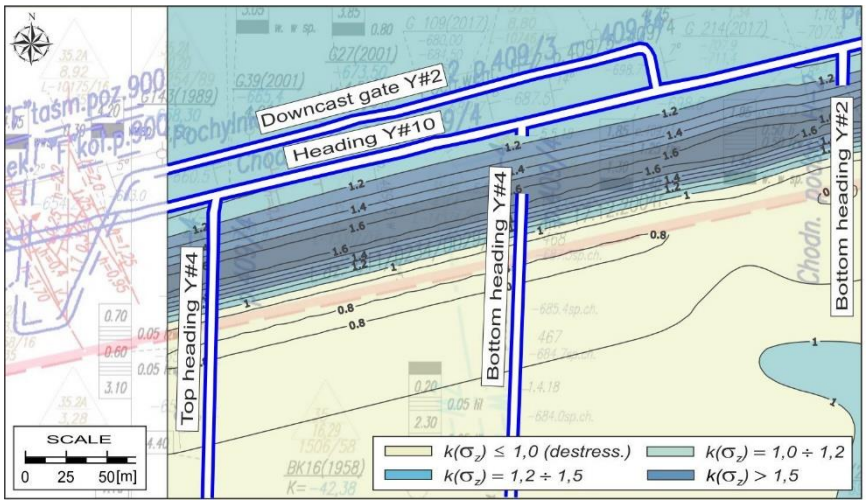

Figure 9. Stress concentration factor (k) in the coal seam (a section of panel Y).

The likelihood of high-energy seismic event incidence at the stage of roadheading operations, associated with the activation of burst-prone strata (sandstones, sandy shales) and with the presence of faults (near the edge of panel Y) is estimated to be minimal. The underlying assumption is that the extent of the state of stress disturbances due to the impacts of the single working face on the surrounding strata should be relatively small and, in most cases, is equal to no more than several widths of the working face. In terms of rockburst risk, which is a resultant of the state of stress and prognosticated seismicity, it is reasonable to expect that rockburst risk during development mining will remain on a medium or locally high level.

4. Discussion

Relevant data and available information on the status and extent of development works in panel Y, coal seam 409-3/4 were synthesised and compiled for the purpose of comparative analysis (Table 2, Figure 10). It was established that seismic hazard levels associated with the roadheading operations (including the drifting of separate segments of a single heading) would vary, both quantitatively and in terms of energy potential. It appears that this state is the result of the prevailing mining conditions associated with previous mining operations in overlying strata, most of all in coal seams 409-3 and 406-1 (Figure 1). In each coal seam in section Y, two longwall panels were operated, their external contours having similar though not fully regular geometry. In the area where the

excavations of concern are located, the mining edges roughly coincide with the southern boundary of the pillar protecting the drift F. The height of the caved-in section in the coal seam 409-3 approaches 3.0 m, in the coal seam 406-1 it is up to 1.6 m, whilst the vertical distance from the coal seam 409-4 is 6–19 m and 150–160 m, respectively.

Table 2. Seismic activity data.

Site	Length (m) /Direction *	N (-) /Energy	As ($\times 10^5$ J)	W1 (m/1 tremor)	W2 (kJ/m)	PN (%)
Heading Y#10	839.0/E	142 10^2–10^4 J	5.05	5.9	0.602	11.3
Downcast gate Y#2	486.0/E	480 10^2–10^5 J	25.00	1.0	5.144	11.0
Top heading Y#4	550.0/S	101 10^2–10^4 J	13.20	5.4 0.8 (70 m)	2.400 18.286^{70m}	41.6
Bottom heading Y#4	512.0 507/N + 5/S	83 61/N, 22/S 10^2–10^4 J	5.34 4.21/N 1.13/S	6.2 0.5 (30 m)	1.043 16.333^{30m}	14.5
Bottom heading Y#2	21.0/S	43 10^2–10^3 J	1.25	0.5	6.098	39.5

* Drivage direction (E—eastwards, N—northwards, S—southwards).

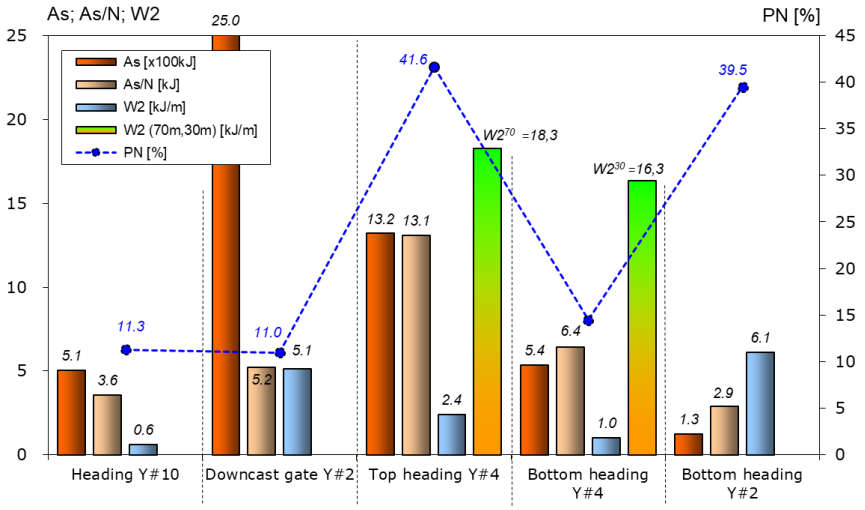

Figure 10. Selected parameters of mining-induced seismicity—comparative diagram.

According to analytical forecasts (Figures 8 and 9), the following two headings were to be completed under similar conditions, in unrelieved zones in which the gravity force remained the major determinant of respective values of the state of stress components:

- Heading Y#10, the forecasted maximal value of vertical stress component ($\sigma_z{}^{max}$) 27.5 MPa (stress concentration factor k^{max} = 1.11);
- Downcast gate Y#2, the forecasted maximal value of vertical stress component ($\sigma_z{}^{max}$) 26.3 MPa (stress concentration factor k^{max} = 1.07).

Even though the downcast gate was decidedly shorter that the heading, increased seismic activity was registered there. The number of seismic events (N) recorded in the course of the drifting operations was 3.4 times larger whilst the registered energy release (As) was nearly 5 times higher in relation to the heading Y#10. On average, a tremor would be registered in the downcast gate Y#2 every 1 m of the work advance (in the heading Y#10 the frequency of tremors would be 5 times smaller), which had a direct impact on the magnitude of generated unit energy (W2). For the downcast gate Y#2, it was found to be equal to 5.1 kJ/m, which was nearly 8 times more than for the heading Y#10 (0.6 kJ/m).

The larger parts of the top and bottom headings Y#4 were driven in strata overcut by working the adjacent seam 409-3 (underneath its goafs). Practically, even though the stress relief conditions ceased because of the time lapse, seismic activity in this area remained on a relatively low level, manifested by few and far between tremors with energy release of the order of 10^3 J. In consideration of dynamic impacts of rock pressure, the most serious problems encountered in mining operations were the drifting and working in the zones (determined by analytical forecasting) impacted by edges of old excavations and previous mining operations in the coal seams 409-3 and 406-1. This observation has relevance to:

- Top heading Y#4 (the initial segment ~70 m in length, in the southward direction), the forecasted maximal vertical stress value ($\sigma_z{}^{max}$) 38.7 MPa (stress concentration factor k^{max} = 1.65);
- Bottom heading Y#4 (the final segment ~25 m in length, in the northward direction and the initial part ~5 m in length, in the southward direction), the forecasted maximal vertical stress value ($\sigma_z{}^{max}$) 39.0 MPa (stress concentration factor k^{max} = 1.64);
- Bottom heading Y#2 (the initial fragment ~20 m in length, driven in the southward direction), the forecasted maximal vertical stress value ($\sigma_z{}^{max}$) 39.6 MPa (stress concentration factor k^{max} = 1.62).

Calculated parameters of mining-induced seismicity in the above-mentioned segments of respective top and bottom headings were found to be unfavourable because the tremors were recorded in this area every 0.8–0.5 m of the working face range, on the average (W1) and the energy released per 1 m of the work advance would fall in the range 6.1–18.3 kJ (W2). Variability of tremor energy in the course of roadheading operations is illustrated by histograms of energy released (Figures 11–13). The advance rate of working faces was not a linear function of time because of certain problems due to recorded seismic activity of rock strata, yet the mine workings of merit are highlighted in the histograms (grey shaded background). Generally, there is a sharp decrease in seismic activity registered in front of the elevated stress zone (bottom heading Y#4) and after leaving it (top heading Y#4), which is revealed by the absence of tremors with the energy potential E $\geq 10^4$ J.

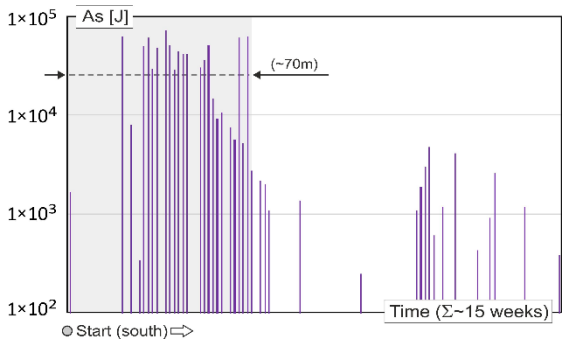

Figure 11. Histogram of seismic energy release—top heading Y#4.

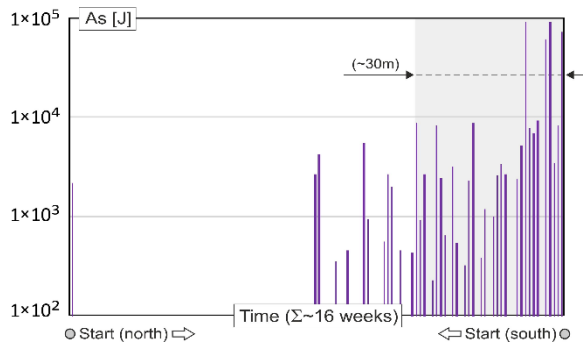

Figure 12. Histogram of seismic energy release—bottom heading Y#4.

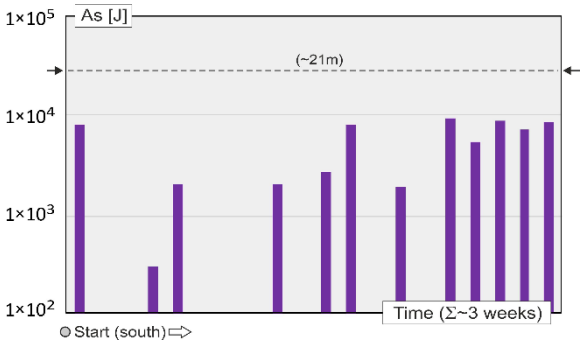

Figure 13. Histogram of seismic energy release—bottom heading Y#2.

It is interesting that the stress concentration zones determined by analytical methods were to be attributed to impacts of the mining edge in a nearby (6–19 m) seam 409-3, which was not verified in the course of repeated in situ tests. During the drifting operations, there were over 700 small-diameter bores that were drilled (∅42 mm, up to 12 m in length) in the coal seam, revealing no critical yield of cuttings (6 dm^3/m). The results of seismoacoustic observations also proved ineffective, 99.5% of them reporting no danger. Yet the technical problem experienced during the mining operations was suggestive of the presence of a zone with unfavourable stress conditions whilst the registered (low-energy) seismic activity indicated the critical state of stress in coal or in the immediate roof or floor strata. Thus, the presented forecast provided an additional (and perhaps the most significant) criterion for the mine operators to rely on when selecting and implementing the rockburst control measures.

In regards to the rockburst protection measures, it appears that the type and extent of deployed control measures were fully adequate to match the hazard levels forecasted and recorded at subsequent stages of the roadheading operation. However, the effectiveness of adopted active control measures (blasting operations, see Table 3) considered in the quantitative analysis of all recorded seismic events (in all energy categories) was found to not be fully satisfactory, averaging 16.5%. One has to bear in mind, however, that the magnitude of rockburst risk is determined by the incidence of high-energy seismic events. It is worthwhile to mention in this regard that 107 (15.9%) tremors with energy potential in the range 10^3–10^4 J were triggered by coal extraction by blasting using small explosive charges (5–7.5 kg of special-purpose metanite).

Table 3. Quantitative proportion of mining-induced events to the number of all recorded events.

Site	N (Nw) with Given Energy			
	10^2 J	10^3 J	10^4 J	10^5 J
Heading Y#10	34 (2 SU)	106 (14 SU)	2	–
Downcast gate Y#2	88 (1 SU)	367 (36 SU)	24 (15 ST)	1 (1 ST)
Top heading Y#4	12 (1 SU)	65 (27 SU)	24 (9 SU, 5 ST)	–
Bottom heading Y#4/N	17 (3 SU)	41 (4 SU)	3	–
Bottom heading Y#4/S	11 (1 SU)	10 (3 SU)	1 (1 ST)	–
Bottom heading Y#2/S	13 (3 SU)	30 (14 SU)	–	–

It was established that concussion (destress) blasting works in the coal seam and torpedo blasting (in roof strata) triggered the occurrence of 31 out of 55 tremors in the energy category 10^4–10^5 J. The overall effectiveness of blasting operations is found to be about 56.4%, which is quite acceptable in terms of rockburst control in underground mines.

5. Conclusions

This study provides an analysis of seismic activity data registered in the course of drifting of five mine headings in a coal seam panel in one of the collieries within the Upper Silesia Coal Basin (Poland), focusing on qualitative and energy indicators characterising seismicity of the rock strata. Calculation parameters, duly summated and averaged, alongside the mapped foci positions, were benchmarked against the analytical forecasts obtained at the stage of design of mining operations. This experiment was conducted to verify the possible correlations between the observed variations of registered seismic activity and anomalies in the state of stress distributions found in model testing. The results lead us to the following general conclusions:

- Seismic hazard associated with roadheading operations in respective headings would vary, both in quantitative terms and in terms of energy potential. Depending on the progress status of the driftage, the number of recorded seismic events would range from 43 to 480. Energy release during the tremors was of the order of 10^5 J.
- According to the analytical forecasts, the state of stress in the investigated coal seam section was non-uniform, revealing the presence of both relieved (destress) zones and the stress-concentration zones. The actual location of anomaly zones was to a large extent associated with the prevailing mining conditions, including the impacts of previous mining operations (exploitation edges, old workings) in the adjacent seams. The horizontal impacts of the edges of coal seams 409-3 and 406-1 extend to about 70 m, covering the area between the downcast gate Y#2 and the southern boundary of the pillar protecting the drift F.
- In terms of totalled values of seismicity parameters, the most extensive seismic activity was registered during the driftage of the downcast gate Y#2. Alongside the entire working range 486 m in length (the shortest fully completed working) 480 seismic events were recorded with the energy potential approaching 2.5×10^6 J. Similar to other workings, the tremors of the order of 10^3 J would be predominant (76.5%) whilst a single tremor of 10^6 J was registered, too.
- Recalling the criteria based on the unit (averaged) calculation parameters, the highest levels of seismic hazard were registered during the driftage of top heading Y#4 (the initial segment ~70 m in length, driven southwards), bottom heading Y#4 (the ultimate segment ~25 m in length, driven northwards and the initial segment ~5 m in length driven southwards), as well as bottom heading Y#2 (the initial segment ~20 m in length driven southwards). Seismic events were few and far between (their energy potential averaging $2.9–13.1 \times 10^3$ J), registered with a frequency of less than 0.8 m of the working face advance, whilst the energy release per one running metre of the driven heading would range from 6.1 to 18.3 kJ.
- Locations of those sections of mine workings where the unit seismicity indicators proved to be the least favourable seem to coincide with stress concentration zones within the coal seam obtained by analytical forecasts, whilst roadheading operations in zones forecasted to be destressed gave rise to decidedly lower seismic activity, both in quantitative terms and in terms of their energy potential.
- Locations of registered rock mass tremor epicentres and foci seem to verify and confirm the adequacy of analytical forecasts predicting locally unfavourable state of stress in the vicinity of mine workings of concern. A lower degree of correspondence between forecast results and seismological data is found for workings driven along the belt-shaped elevated stress zone (heading Y#10, downcast gate Y#2).
- Unfavourable stress conditions in the coal seam are revealed by the rock strata response to active rockburst control measures. Concussion and destress blasting operations in the coal strata triggered the incidence of about 16% seismic events with energy potential in the range $10^3–10^4$ J (79% of the entire population of recorded tremors). Tremors were found to have been more readily triggered in the stress concentration zones determined by analytical modelling.

In the light of the above conclusions it is reasonable to state that the adopted analytical modelling of the state of stress might be well employed in engineering practice as a valuable tool for supporting the forecasting (at the stage of work design) and verification of predicted seismic hazard levels (at the stage of mining operations). However, due to complexity of geological and mining conditions within the Upper Silesia Coal Basin and to variability of geomechanical parameters of the rock strata, the forecast ought to be full and comprehensive, taking into account the assessments of the rock mass conditions by diverse methods (including the mining and geophysical methods).

Author Contributions: (D.C.): research/paper idea, data analysis and verification, stress state analytical modelling, results comparison, conclusions and final editing; (Z.B.): data collecting and preliminary analysis, seismicity parameters calculation/processing, results visualisation and draft text editing. Both authors have read and agreed to the published version of the manuscript.

Funding: The article was funded by AGH University of Science and Technology, Faculty of Civil Engineering and Resource Management (subsidy no. 16.16.100.215).

Institutional Review Board Statement: Not applicable.

Informed Consent Statement: Not applicable.

Data Availability Statement: The data analysed in the article are available on request from the corresponding author (not publicly available).

Conflicts of Interest: The authors wish to confirm that there is no known conflict of interest associated with this publication.

References

1. Brady, B.H.G.; Brown, E.T. *Rock Mechanics for Underground Mining*; Springer: Dordrecht, The Netherlands, 1994.
2. Gil, H. *The Theory of Strata Mechanics*; Wydawnictwo PWN: Warszawa, Poland, 1991.
3. Sałustowicz, A. *Fundamentals of Strata Mechanics*; Wydawnictwo Śląsk: Katowice, Poland, 1968; p. 196. (In Polish)
4. Barański, A.; Drzewiecki, J.; Kabiesz, J.; Konopko, W.; Kornowski, J.; Krzyżowski, A.; Mutke, G.; Dubiński, J.; Lurka, A.; Stec, K.; et al. *Guidelines for Application of the Comprehensive Method and Specific Methods for Rockburst Hazard Assessment in Coal Mines*; no 20, 22; Wydawnictwo GIG: Katowice, Poland, 2012. (In Polish)
5. Zhou, J.; Li, X.; Mitri, H.S. Evaluation method of rockburst: State-of-the-art literature review. *Tunn. Undergr. Space Technol.* **2018**, *81*, 632–659. [CrossRef]
6. Adamczewski, Z.; Larsen, L. Technology for determining days of active seismicity. *Przegląd Geod.* **2002**, *9*, 3–8. (In Polish)
7. Goszcz, A. Seismic Hazard-Selected Aspects (a Controversial Paper). 2003. Available online: https://doczz.pl/doc/2687350/antoni-goszcz-kilka-uwag-o-zagro%C5%BCeniu-sejsmicznym (accessed on 1 September 2021). (In Polish).
8. Kłeczek, Z. Control of Rock-Mass Bursts in Polish Copper Mines. 2007. Available online: https://doczz.pl/doc/1563269/zdzis%C5%82aw-k%C5%82eczek-sterowanie-wstrz%C4%85sami-g%C3%B3rotworu-lgom (accessed on 1 September 2021). (In Polish)
9. Kornowski, J.; Kurzeja, J. Short-term forecasts of mining-induced seismic hazard. *Res. Rep. Min. Environ.* **2005**, *1*, 33–48.
10. Gibowicz, S.J. Seismicity induced by mining recent research. *Adv. Geophys.* **2009**, *51*, 1–53.
11. Hatherly, P. Overview on the application of geophysics in coal mining. *Int. J. Coal Geol.* **2013**, *114*, 74–84. [CrossRef]
12. Lasocki, S. Probabilistic seismic hazard analysis for mining-induced seismicity. In Proceedings of the 7th International Symposium on Rockbursts and Seismicity in Mines (RaSiM7), Dalian, China, 21–23 August 2009; pp. 59–72.
13. Wesseloo, J. Towards real-time probabilistic hazard assessment of the current hazard state for mines. In Proceedings of the 8th International Symposium on Rockbursts and Seismicity in Mines (RaSiM8), Moscow, Russia, 1–7 September 2013; pp. 307–312.
14. Kornowski, J. Linear prediction of hourly aggregated AE and tremors energy emitted from a longwall and its performance in practice. *Arch. Min. Sci.* **2003**, *48*, 315–337.
15. Cianciara, A.; Cianciara, B. The meaning of seismoacoustic emission for estimation of time of mining tremors occurrence. *Arch. Min. Sci.* **2006**, *51*, 563–575.
16. Caputa, A.; Rudziński, Ł. Synthetic tests of full waveform inversion with configuration of Rudna mine real seismic monitoring system. *Przegląd Geofiz.* **2020**, *3–4*, 123–138.
17. Hosseini, N. Evaluation of the rockburst potential in longwall coal mining using passive seismic velocity tomography and image subtraction technique. *J. Seismol.* **2017**, *21*, 1101–1110. [CrossRef]
18. Mutke, G.; Dubiński, J.; Lurka, A. New criteria to assess seismic and rockburst hazard in coal mines. *Arch. Min. Sci.* **2015**, *60*, 743–760.
19. Mutke, G.; Pierzyna, A.; Barański, A. b-value as a criterion for the evaluation of rockburst hazard in coal mines. In Proceedings of the 3rd International Symposium on Mine Safety Science and Engineering (ISMS), Montreal, QC, Canada, 13–19 August 2016; pp. 1–5.

20. Cichy, T.; Prusek, S.; Świątek, J.; Apel, D.B.; Yuanyuan Pu, Y. Use of neural networks to forecast seismic hazard expressed by number of tremors per unit of surface. *Pure Appl. Geophys.* **2020**, *177*, 5713–5722. [CrossRef]
21. Geng, Y.; Su, L.; Jia, Y.; Han, C. Seismic events prediction using deep temporal convolution networks. *J. Electr. Comput. Eng.* **2019**, *2019*, 7343784. [CrossRef]
22. Kabiesz, J.; Sikora, B.; Sikora, M.; Wróbel, Ł. Application of rule-based models for seismic hazard prediction in coal mines. *Acta Montan. Slovaca* **2013**, *18*, 262–277.
23. Pu, Y.; Apel, D.B.; Liu, V.; Mitri, H. Machine learning methods for rockburst prediction-state-of-the-art review. *Int. J. Min. Sci. Technol.* **2019**, *29*, 565–570. [CrossRef]
24. Kurzeja, J.; Kornowski, J. The basic assumptions of the quantitative version of the comprehensive method of rockburst hazard evaluation. *Miner. Resour. Manag.* **2013**, *29*, 193–204. [CrossRef]
25. *Regulation by the Minister for Energy on Specific Requirements Having Relevance to Underground Mining Operations*; Ministry of Energy: Warszawa, Poland, 2017; p. 393. (In Polish)
26. Patyńska, R. Mining-geologic conditions of extraction of seams under rockburst hazard in the period 1987–2007. *Gospod. Surowcami Miner.* **2008**, *24*, 227–243. (In Polish)
27. The mine's natural hazards department. The comprehensive project of rockburst hazard deposit exploitation. *Unpublished work*, 2018. (In Polish)
28. Gibowicz, S.J.; Kijko, A. *An Introduction to Mining Seismology*; Academic Press: Cambridge, MA, USA, 1994.
29. Gibowicz, S.J.; Lasocki, S. Seismicity induced by mining: Ten years later. *Adv. Geophys.* **2001**, *44*, 39–181.
30. Glazer, S.N. *Mine Seismology: Seismic response to the Caving Process*; Springer Publishers: Cham, Switzerland, 2018; p. 242.
31. Mendecki, A.J. *Seismic Monitoring in Mines*; Chapman & Hall: London, UK, 1997.
32. Bracławska, A.; Idziak, A.F. Study on energy distributions of strong seismic events in the USCB. *Contemp. Trends Geosci.* **2017**, *6*, 41–56. [CrossRef]
33. Mendecki, M.J.; Wojtecki, Ł.; Zuberek, W.M. Case studies of seismic energy release ahead of underground coal mining before strong tremors. *Pure Appl. Geophys.* **2019**, *176*, 3487–3508. [CrossRef]
34. Stec, K.; Lurka, A. Characteristics and seismological methods of seismic activity analysis. *Przegląd Górniczy* **2015**, *71*, 83–93. (In Polish)
35. Wojtecki, Ł.; Kurzeja, J.; Knopik, M. The influence of mining factors on seismic activity during longwall mining of a coal seam. *Int. J. Min. Sci. Technol.* **2021**, *31*, 429–437. [CrossRef]
36. Schreiber, J.; Konicek, P.; Stonis, M. Seismological activity during room and pillar hard coal extraction at great depth. *Procedia Eng.* **2017**, *191*, 67–73. [CrossRef]
37. Van Dyke, M.A.; Su, W.H.; Wickline, J. Evaluation of seismic potential in a longwall mine with massive sandstone roof under deep overburden. *Int. J. Min. Sci. Technol.* **2018**, *28*, 115–119. [CrossRef]
38. Zhang, M.; Shimada, H.; Sasaoka, T.; Matsui, K. Seismic energy distribution and hazard assessment in underground coal mines using statistical energy analysis. *Int. J. Rock Mech. Min. Sci.* **2013**, *64*, 192–200. [CrossRef]
39. Van Aswegen, G. Routine seismic hazard assessment in some South African Mines. *Int. Symp. Rockburst Seism. Mines* **2005**, 1–10. [CrossRef]
40. Ahn, K.S.; Zhang, C.G.; Canbulat, I. Study of seismic activities associated with Australian underground coal mining. In Proceedings of the 17th Coal Operators' Conference, Wollongong, Australia, 8–10 February 2017; pp. 275–282.
41. Bischoff, M.; Cete, A.; Fritschen, R.; Meier, T. Coal mining induced seismicity in the Ruhr area (Germany). *Pure Appl. Geophys.* **2010**, *167*, 63–75. [CrossRef]
42. Dineva, S.; Boskovic, M. Evolution of seismicity at Kiruna Mine. In Proceedings of the Eighth International Conference on Deep and High Stress Mining, Perth, Australia, 28–30 March 2017; pp. 125–139.
43. Mansurov, V.A. Prediction of rockbursts by analysis of induced seismicity data. *Int. J. Rock Mech. Min. Sci.* **2001**, *38*, 893–901. [CrossRef]
44. Srinivasan, C.; Arora, S.K.; Yaji, R.K. Use of mining and seismological parameters as premonitors of rockbursts. *Int. J. Rock Mech. Min. Sci.* **1997**, *34*, 1001–1008. [CrossRef]
45. Dymek, F. Boundary problem in terms of displacement in a 3D theory of elasticity and its applications to strata mechanics. *Arch. Min. Sci.* **1969**, *3*, 263–280. (In Polish)
46. Ozog, T. Roof subsidence taking into account shearing forces. *Zesz. Probl. Górnictwa PAN* **1965**, *3*, 45–79. (In Polish)
47. Bańka, P.; Jaworski, A.; Plewa, F. Assessment of quake and rockburst hazard in underground mines by analytical methods. *Przegląd Górniczy* **2012**, *68*, 13–19. (In Polish)
48. Kłeczek, Z.; Małoszewski, J.; Parysiewicz, S.; Zorychta, A. *Geomechanical Criteria of Rockburst Hazard during Exploitation of Hard Coal Seams*; Wydawnictwo GIG: Katowice, Poland, 1987. (In Polish)
49. Pietuchow, I.M.; Linkov, M.A. The theory of post-failure deformations and the problem of stability in rock mechanics. *Int. J. Rock Mech. Min. Sci. Geomech. Abstr.* **1979**, *16*, 57–76.
50. Yang, J.; Chen, W.; Tan, X.; Yang, D. Analytical estimation of stress distribution in interbedded layers and its implication to rockburst in strong layer. *Tunn. Undergr. Space Technol.* **2018**, *81*, 289–295. [CrossRef]
51. Zorychta, A. *Geomechanical Models of Bursting Rock Mass*; Wydawnictwo IGSMiE PAN: Kraków, Poland, 2003. (In Polish)

52. *Regulation by the Minister of Environment on Natural Hazards in Mines*; Ministry of Environment: Warszawa, Poland, 2013; p. 20. (In Polish)
53. Chlebowski, D. *Analytical Modeling of Constrained Exploitation in the Aspect of Identification of Rockburst Hazard Areas, no. 290*; Wydawnictwo AGH: Kraków, Poland, 2013. (In Polish)
54. Kłeczek, Z. *Mining Geomechanics*; Śląskie Wydawnictwo Techniczne: Katowice, Poland, 1994. (In Polish)
55. Chlebowski, D. The influence of selected geomechanical parameters on the formation of vertical displacements and stresses in the vicinity of the fault. *Przegląd Górniczy* **2009**, *65*, 1–7. (In Polish)
56. Kłeczek, Z.; Zorychta, A. Influence of the exploitation remnants on the stress state of the rock mass at risk of rockburst. *Zesz. Nauk. Politech. Śląskiej Górnictwo* **1990**, *185*, 7–34. (In Polish)
57. Zorychta, A.; Chlebowski, D. Influence of selected natural and technological parameters on the rockburst hazard in the conditions of exploitation remnants. *Pr. Nauk. GIG* **1998**, *26*, 149–164. (In Polish)